

Experimental study on performance of 100-kW low temperature superconducting steady-state magnetoplasmadynamic thruster

Cheng Zhou(周成), Peng Wu(吴鹏), Yun-Tao Song(宋云涛), Jin-Xing Zheng(郑金星), Yong Li(李永), Ge Wang(王戈), and Hai-Yang Liu(刘海洋)

Citation: Chin. Phys. B, 2025, 34 (**2**): 025201. DOI: 10.1088/1674-1056/ad9910
Journal homepage: http://cpb.iphy.ac.cn; http://iopscience.iop.org/cpb

What follows is a list of articles you may be interested in

Temporal variation characteristics of cathode temperature in a magnetoplasmadynamic thruster

Cheng Zhou(周成), Peng Wu(吴鹏), Yun-Tao Song(宋云涛), Jin-Xing Zheng(郑金星), Yong Li(李永), Ge Wang(王戈), and Hai-Yang Liu(刘海洋)
Chin. Phys. B, 2025, 34 (**2**): 025202. DOI: 10.1088/1674-1056/ad9e9b

Growth mechanism and characteristics of electron drift instability in Hall thruster with different propellant types

Long Chen(陈龙), Zi-Chen Kan(阚子晨), Wei-Fu Gao(高维富), Ping Duan(段萍), Jun-Yu Chen(陈俊宇), Cong-Qi Tan(檀聪琦), and Zuo-Jun Cui(崔作君)
Chin. Phys. B, 2024, 33 (**1**): 015203. DOI: 10.1088/1674-1056/acf9e5

Interaction between plasma and electromagnetic field in ion source of 10 cm ECR ion thruster

Hao Mou(牟浩), Yi-Zhou Jin(金逸舟), Juan Yang(杨涓), Xu Xia(夏旭), and Yu-Liang Fu(付瑜亮)
Chin. Phys. B, 2022, 31 (**7**): 075202. DOI: 10.1088/1674-1056/ac4906

Research of influence of the additional electrode on Hall thruster plume by particle-in-cell simulation

Xi-Feng Cao(曹希峰), Hui Liu(刘辉), Da-Ren Yu(于达仁)
Chin. Phys. B, 2020, 29 (**9**): 095204. DOI: 10.1088/1674-1056/aba2e3

The *E*×*B* drift instability in Hall thruster using 1D PIC/MCC simulation

Zahra Asadi, Mehdi Sharifian, Mojtaba Hashemzadeh, Mahmood Borhani Zarandi, Hamidreza Ghomi Marzdashti
Chin. Phys. B, 2020, 29 (**2**): 025204. DOI: 10.1088/1674-1056/ab6719

Experimental study on performance of 100-kW low temperature superconducting steady-state magnetoplasmadynamic thruster

Cheng Zhou(周成)[1,2,3], Peng Wu(吴鹏)[3], Yun-Tao Song(宋云涛)[1,2], Jin-Xing Zheng(郑金星)[1,2], Yong Li(李永)[3,†], Ge Wang(王戈)[3], and Hai-Yang Liu(刘海洋)[2]

[1] *University of Science and Technology of China, Hefei* 230031, *China*
[2] *Hefei Institutes of Physical Science, Chinese Academy of Sciences, Hefei* 230031, *China*
[3] *Beijing Institute of Control Engineering, Beijing* 100080, *China*

(Received 26 September 2024; revised manuscript received 26 November 2024; accepted manuscript online 2 December 2024)

Applied field magnetoplasmadynamic thrusters (AF-MPDTs), with their high specific impulse and considerable thrust, are increasingly favored for large-scale space missions. This paper presents the composition, functionality, and testing methods of a high-power electric propulsion performance testing system, along with the vacuum ignition test results of a 100 kW superconducting MPD thruster. The relationships between thruster efficiency, magnetic field strength, current, and mass flow rate are analyzed. For each combination of current and flow rate in an AF-MPDT, there is an optimal magnetic field strength where the thruster efficiency reaches its peak. Under conditions of 320 A current and 60 mg/s flow rate, the optimal magnetic field strength is 0.5 T, yielding the highest thruster efficiency of 71%.

Keywords: magnetoplasmadynamic thruster, high-power electric propulsion, superconduction, performance measurements

PACS: 52.75.Di, 85.70.Rp

DOI: 10.1088/1674-1056/ad9910 **CSTR:** 32038.14.CPB.ad9910

1. Introduction

Large-scale deep space exploration missions, such as Earth–Moon cargo transport and rapid manned Mars exploration, impose stringent demands on propulsion systems, particularly in terms of velocity increment. Traditional chemical propulsion systems, while capable of delivering high thrust, are constrained by low specific impulse and high propellant consumption, thereby reducing the spacecraft's payload capacity.[1–5] In contrast, low-power electric propulsion systems offer high specific impulse but generate insufficient thrust, leading to extended orbital transfer durations. This highlights the urgent need for the development of high-power electric propulsion technologies that strike a balance between high thrust, high specific impulse, and long operational life.

The applied field magnetoplasmadynamic thruster (AF-MPDT) is an advanced electromagnetic propulsion device that generates high-density plasma by ionizing the working medium through a high-temperature arc, and produces thrust by accelerating the plasma via the Lorentz force created by a combination of a strong magnetic field and high current.[6,7] This technology offers several key advantages, including high power output, ultra-high specific impulse, high thrust density, compact size, and low weight. As a result, it can efficiently deliver the propulsion required for tasks such as large-scale orbital transfers.

Leading space-faring nations, including the United States, Russia, Germany, and Japan, are actively advancing research on steady-state magnetoplasmadynamic thruster technology.[8–10] Test systems currently operate at power levels ranging from 20 kW to 500 kW, with specific impulse values between 2000 s and 9410 s, and efficiencies varying from 20% to 90%. With a common goal of achieving higher power, efficiency, and specific impulse, these countries are engaged in comprehensive design and prototype development efforts aimed at creating more advanced high-power MPDT.

In 2018, leveraging the performance insights gained from the SX3 thruster at the University of Stuttgart and advancements in high-temperature superconducting technology by THEVA, German PI Integral Solutions outlined the technical development requirements for high-power MPD thrusters intended for on-orbit applications. Subsequently, in 2019, the SUPREME thruster, based on the SX3 design, was proposed.[11,12] This plan involves utilizing high-temperature superconducting magnets to develop a 50 kW superconducting MPD thruster, featuring a magnetic field strength of 0.8–1.5 T, a thrust of 1300 mN, a specific impulse of 4000 s, and an efficiency of 65% (using argon as the propellant). Future developments include the design and construction of a 100 kW thruster. Voronov reported the results of an AF-MPDT study based on second-generation high-temperature superconductor (2G HTS) tape technology. The best performance metrics achieved include a thrust of up to 850 mN, a specific impulse of up to 3840 s, and an efficiency of up to 54%.[10]

[†]Corresponding author. E-mail: 18510489511@163.com

© 2025 Chinese Physical Society and IOP Publishing Ltd. All rights, including for text and data mining, AI training, and similar technologies, are reserved.

This paper presents the results of vacuum ignition tests on a 100 kW superconducting steady-state AF-MPDT. The relationships between thruster efficiency, magnetic field strength, current, and mass flow rate are analyzed. Current efforts are focused on the development of a miniaturized high-temperature superconducting stable magnetic plasma thruster, laying the technical foundation for future on-orbit applications.

2. Testing system

2.1. System composition and layout

The configuration of the high-power magnetoplasmadynamic (MPD) vacuum ignition test system is illustrated in Fig. 1, consisting of five primary subsystems: the vacuum system, power source system, propellant supply system, water-cooling system, and target thrust measurement system. The vacuum system establishes the necessary environment for thruster ignition, maintaining an ultimate vacuum pressure of 10^{-4} Pa. The power source system supplies ignition, excitation, and anode power to the thruster while monitoring electrical parameters, including steady-state discharge voltage and current, excitation coil voltage and current, as well as arc initiation voltage and current. The propellant supply system delivers argon to the thruster cathode at a flow rate of 0–150 mg/s. The water-cooling system circulates deionized water to the thruster's anode, cathode, and excitation coils for cooling, while also monitoring temperature data from six inlet and outlet pipes, as well as the anode shell and cathode components. Lastly, the target thrust measurement system measures the thrust produced by the thruster, with a measurement range of 0.1 N to 10 N.

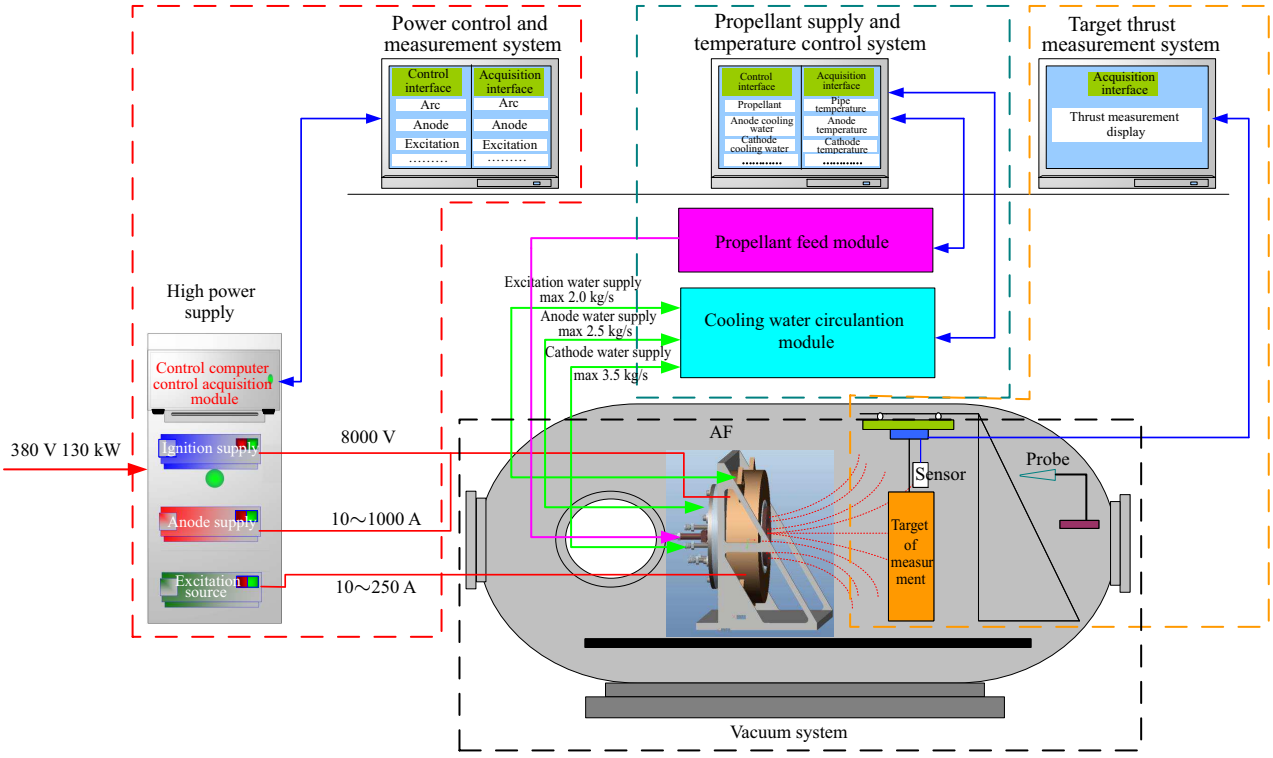


Fig. 1. Composition diagram of ignition test system for high-power MPDT.

2.2. Main experimental equipment

The high-power electric propulsion vacuum test system is primarily composed of large-scale vacuum equipment devices, including a large vacuum tank, three cryogenic vacuum pump systems with ultra-high pumping speeds, six xenon vacuum pump systems, two high-power molecular pump systems, high-power vacuum roots pump systems, a large-scale ultra-high pumping speed central control system, and fully elastic directional thermal deformation compensation devices. To maintain the vacuum environment necessary for high-power MPD ignition, ranging from 10^{-1} Pa to 10^{-4} Pa, all three cryogenic pumps can be activated simultaneously. Under an argon flow rate of 60 mg/s, the ambient pressure can be maintained below 0.1 Pa. Additionally, the vacuum system is equipped with a beam protection system to mitigate the sputtering of xenon particles during ignition. This beam protection system features a heat sink-like structure, with all components made of titanium, as shown in Fig. 2.

The power source system provides high-voltage ignition pulses, anode power, and excitation power for the startup of the electromagnetic thruster, while also ensuring its stable operation and thrust generation. This system utilizes advanced

switching power supply technology based on high-frequency inverters and is equipped with a high-frequency trigger system. Operating in constant current control mode, it includes features for setting power supply states, input/output index testing, and fault protection mechanisms against issues such as water shortages, overvoltage, overcurrent, and overheating. The power source system consists of an arc-starting power supply, anode power supply, excitation power supply, internal controller, switch panel, remote controller, testing tools, equipment cabinet, and cooling system. The thruster power source provides a direct current of up to 1000 A and max discharge voltage of 250 V. The coil power source provides a direct current of up to 250 A. The discharge voltage and the thrust signal are acquired by the GEN2i data acquisition of HBM.



Fig. 2. View of large vacuum system and beam protection plate.

2.3. Low temperature superconducting AF-MPDT

The configuration of the AF-MPD thruster used in this test is illustrated in Fig. 3. It primarily consists of five components: the cathode, anode, insulation structure, water-cooled structure, and superconducting magnet.



Fig. 3. View of low temperature superconducting MPD thruster.

The superconducting magnet features an inner diameter of 173 mm, an outer diameter of 357.2 mm, and a thickness of 167.4 mm, with a design maximum magnetic field strength of 2.0 T. The superconducting coil, along with its supporting coil box and G10 thermal insulation material, forms a cohesive unit, as illustrated in Fig. 4. During normal operation, the internal temperature must not exceed the superconducting coil conductor's critical temperature, which is generally maintained below 4.2 K. The superconducting coil is suspended within a cryogenic Dewar. To ensure stable operation at the liquid helium temperature of 4.2 K, various factors including self-weight, electromagnetic forces, and thermal stress must be carefully considered in the design of the internal structure.

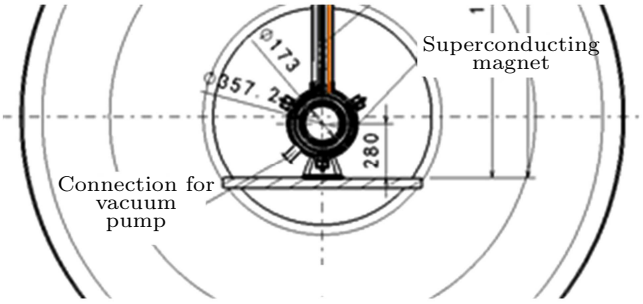


Fig. 4. Schematic diagram of class T superconducting coil.

The primary structure of the MPD thruster consists of a magnet, cathode, and anode, along with additional components such as insulation and sealing structures. To achieve a compact overall design while ensuring structural integrity and ease of assembly, efforts are made to minimize both axial and radial dimensions of the components. TC4 titanium alloy is used for the cathode and anode connectors, while boron nitride ceramic serves as the insulating material in high-temperature regions. The cylindrical anode features a water-cooling structure to dissipate heat from its surface, with inner and outer diameters of 60 mm and 165 mm, respectively, and a length of 30 mm. Propellant is injected solely through the cathode, which is made of tungsten, measuring 10 mm in length (within the discharge chamber) and 24 mm in diameter. The cathode includes nine channels, each with a diameter of 3 mm, and is housed within a water-cooled copper structure.

3. Measuring method

Thrust is measured using a thrust target, as illustrated in Figs. 5 and 6. The thrust measurement system includes a circular graphite target with a diameter of 600 mm, an ILD 1700-10 laser displacement sensor, an elastic beam, and a displacement mechanism. Thrust is determined by measuring the target's displacement with the laser sensor. In this thrust measurement setup, the elastic beam, rigid target, and displacement sensor operate in concert, with the rigid target affixed to the lower end of the elastic beam. The force exerted by the beam causes deformation of the target surface, while the displacement sensor captures the beam's shape variations. Thrust is then calculated using the calibration curve of the thrust frame. The thrust target measurements are affected by the distance between the target surface and the thruster. In this study, the maximum thrust target measurement was used to represent the thrust of the AF-MPDT. This measurement methodology has been previously published in Refs. [13,14].

In order to know the accurate relationship between the output signal and the real force, five weights with different masses were used as the standard force to calibrate the target thrust stand. The thrust stand was calibrated four times before the experiment and the calibration results are shown in Fig 7.

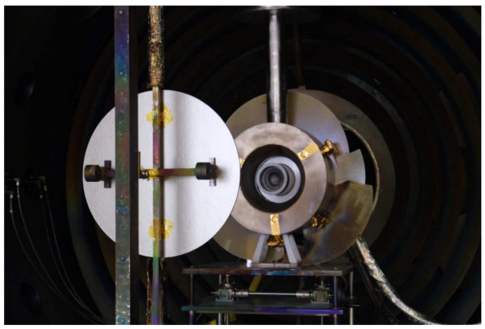


Fig. 5. View of thrust measurement of low temperature superconducting MPD thruster by shooting method.

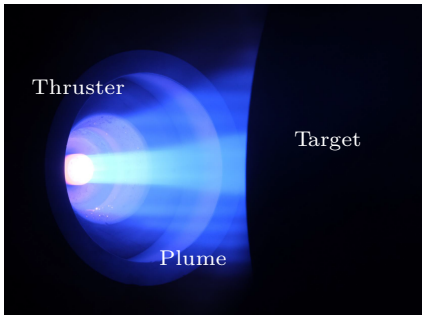


Fig. 6. The target thrust measurement.

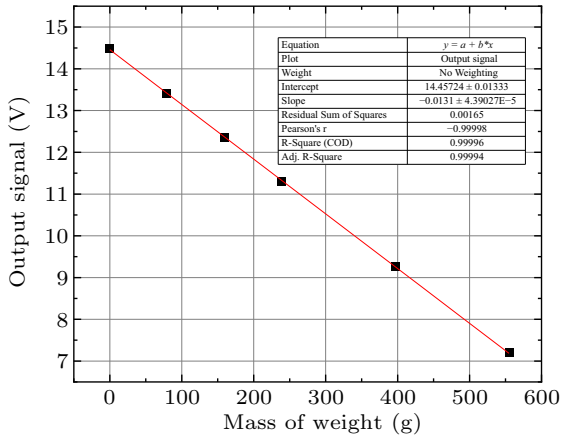


Fig. 7. The calibration curve for the target thrust stand with weights.

4. Test results and analysis

All test data are collected by the data acquisition, which measures thrust, voltage, current, flow, and magnetic field strength. The specific impulse and efficiency of the thruster are derived from these measurements. The derivation process for specific impulse is given by

$$I_{\mathrm{SP}} = \frac{T}{g_0 \dot{m}}, \tag{1}$$

where g_0 is the acceleration of gravity, $\dot{m}$ is the mass flow, and T is the thrust of the thruster. The efficiency derivation process is shown below:

$$\eta = \frac{T^2}{2\dot{m}P} = \frac{T^2}{2\dot{m}U_{\mathrm{a}}I_{\mathrm{a}}}, \tag{2}$$

where P is the output power of the thruster, U_{a} is the anode voltage of the thruster, and I_{a} is the working current of the thruster. In practice, the power consumption of the superconducting magnet is two orders of magnitude lower than the actual operating power of the thruster; therefore, the power calculated for efficiency does not include the power of the superconducting magnet.

Figure 8 illustrates the relationship between the efficiency, voltage, and magnetic field strength of the thruster. As the magnetic field strength increases, the anode voltage of the thruster also rises. Notably, when the magnetic field strength is between 0.6 T and 0.65 T, the voltage growth rate increases significantly. The efficiency of the thruster initially rises with increasing magnetic field strength, reaching a maximum value of 71% at 0.53 T. However, beyond this point, further increases in magnetic field strength lead to a decrease in efficiency. When the magnetic field exceeds 0.5 T, the efficiency increases with the rising magnetic field strength. This phenomenon may be attributed to the anode starvation effect. As the magnetic field strength increases, the plasma is compressed towards the cathode, resulting in a depletion of charge carriers near the anode. This depletion is insufficient to sustain the discharge current, necessitating an increase in the potential drop near the anode to maintain discharge. Consequently, this leads to an increase in anode power deposition, which ultimately results in a decrease in efficiency.[15–17]

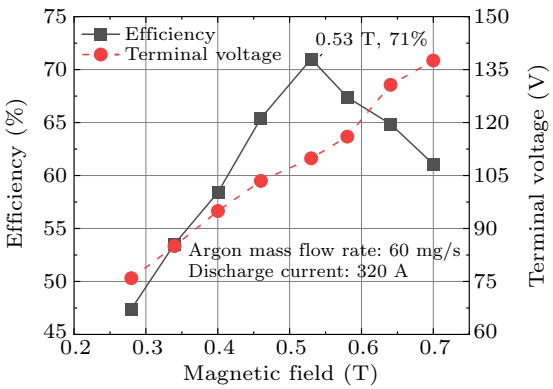


Fig. 8. Change curve of thruster voltage and efficiency with magnetic field strength.

Figure 9 presents the relationship between thruster voltage, efficiency, and current. When the working current ranges from 320 A to 400 A, the thruster efficiency increases significantly and linearly with the current. Between 400 A and 570 A, the efficiency rises more slowly, with diminishing increments, ultimately stabilizing at approximately 68% efficiency. Additionally, when the working current is between 320 A and 450 A, the thruster voltage increases nonlinearly with current. From 450 A to 575 A, the voltage rises slowly and linearly. The maximum power of the thruster in this study reached 50 kW, whereas the current maximum power of superconducting AF-MPDTs was 25 kW.[10]

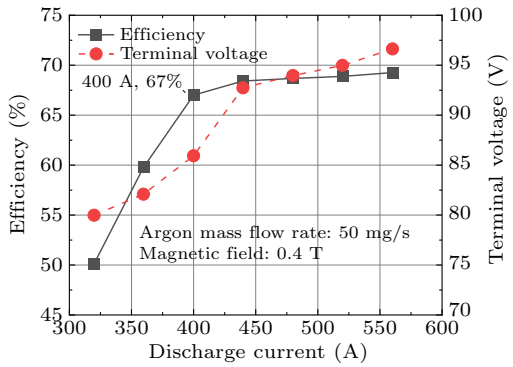


Fig. 9. Change curve of thruster voltage and efficiency with current.

Figure 10 illustrates the relationship between thruster efficiency, voltage, and flow rate. As the flow rate increases, the anode voltage of the thruster decreases. The efficiency initially rises with increasing flow rate, reaching a maximum value of 60% at a flow rate of 35 mg/s. However, further increases in flow rate lead to a rapid decline in thruster efficiency. Under certain current and magnetic field conditions, the efficiency first increases and then decreases with the rise in propellant flow rate. This behavior is caused by two factors. Initially, the increase in flow rate alleviates the anode starvation effect under these operating conditions. However, when the flow rate exceeds the operational limit, the energy used for acceleration is diverted towards ionizing the excess injected propellant, which ultimately leads to a reduction in efficiency.

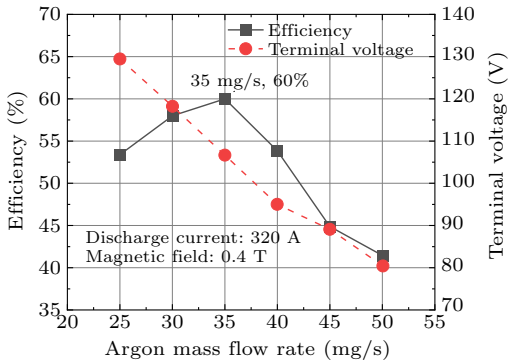


Fig. 10. Change curve of thruster voltage and efficiency with mass flow rate.

5. Conclusion

The applied field magnetoplasmadynamic thruster (AF-MPDT) is recognized as one of the most promising propulsion systems for deep space exploration. Extensive research has been conducted to investigate the performance of AF-MPDTs. This paper presents the performance characteristics of a 100 kW superconducting MPD thruster, with the following key conclusions.

With a propellant flow rate of 60 mg/s and an anode current of 320 A, the thruster's anode voltage increases with the magnetic field strength. Notably, the voltage growth rate experiences a significant spike when the magnetic field strength is between 0.6 T and 0.65 T. The thruster's efficiency initially rises with the increasing magnetic field strength, reaching a peak of 71% at a magnetic field strength of 0.53 T. However, further increases in magnetic field strength result in a decline in efficiency.

At a propellant flow rate of 50 mg/s and a magnetic field strength of 0.4 T, the thruster exhibits a linear increase in efficiency as the working current rises from 320 A to 400 A. As the current continues to increase beyond this range, the efficiency continues to rise, but at a slower rate, with diminishing increments. Eventually, the efficiency stabilizes at approximately 68%, showing little variation thereafter.

The propellant flow rate increases, the anode voltage decreases, and the thruster efficiency initially improves, reaching a peak efficiency of 60% at a flow rate of 35 mg/s. Beyond this threshold, further increases in flow rate result in a rapid decline in efficiency.

Although this study presents experimental investigations on low-temperature superconducting AF-MPDTs, it is important to acknowledge that low-temperature superconducting technology presents certain challenges for space applications. Future research will focus on the development and study of high-temperature superconducting AF-MPDTs. Additionally, direct thrust measurements will be performed using a fully elastic thrust stand, with the results compared and validated against those obtained from the target thrust stand.

References

[1] Auweter-Kurtz M, Kriille G and Kurtz H 1997 *The Investigation of Applied-Field MPD Thrusters on the International Space Station The 25th International Electric Propulsion Conference* (Cleveland, Ohio: Electric Rocket Propulsion Society) p. 721
[2] Russell C T, Abshire J and A'Hearn M 1996 *Advances in Space Research* **18** 75
[3] Zhang Z, Zhao Z, Liu X and Wang N 2024 *Chinese Journal of Aeronautics* **37** 38
[4] Li X K, Che B X, Cheng M S, Guo D W, Wang M G and Yang Y T 2020 *Chin. Phys. B* **29** 115201
[5] Mou H, Jin Y Z, Yang J, Xia X and Fu Y L 2022 *Chin. Phys. B* **31** 075202
[6] Wu P, Wang Y, Li Y, Zhou C, Wang Y, Chen Z, Han X and Tang H 2022 *Acta Astronautica*
[7] Kumar Meena L, Anand A and Gour A S 2022 *IOP Conference Series: Materials Science and Engineering* **1240** 012002
[8] Sasoh A, Mizutani K and Iwakawa A 2017 *AIP Advances* **7** 065204
[9] Sasoh A and Arakawa Y 1992 *Journal of Propulsion and Power* **8** 98
[10] Voronov A S, Troitskiy A A, Egorov I D, Samoilenkov S V and Vavilov A P 2020 *Journal of Physics: Conference Series* **1686** 012023
[11] Boxberger A, Behnke A and Herdrich G *2019 Current Advances in Optimization of Operative Regimes of Steady State Applied Field MPD Thrusters The 36th International Electric Propulsion Conference* (University of Vienna, Austria: Electric Rocket Propulsion Society) p. 585
[12] Boxberger A and Herdrich G 2017 *Integral measurements of 100 kW class steady state applied-field magnetoplasmadynamic thruster SX3 and perspectives of AF-MPD technology The 35th International Electric Propulsion Conference* (Georgia Institute of Technology, Atlanta, Georgia, USA: Electric Rocket Propulsion Society) p. 339
[13] Wang B, Tang H, Wang Y, Lu C, Zhou C, Dong Y, Wang G, Cong Y, Luu D and Cao J 2018 *Jove-Journal of Visualized Experiments* **2** 20
[14] Wang B, Yang W, Tang H, Li Z, Kitaeva A, Chen Z, Cao J, Herdrich G and Zhang K 2018 *Measurement Science and Technology* **29** 075302
[15] Gallimore A D, Kelly A J and Jahn R G 1993 *Journal of Propulsion and Power* **9** 361
[16] Gallimore A D, Myers R M, Kelly A J and Jahn R G 1994 *Journal of Propulsion and Power* **10** 262
[17] Dinulescu H A and Pfender E 1980 *J. Appl. Phys.* **51** 3149